New Free-Wake Analysis of Rotorcraft Hover Performance Using Influence Coefficients

Todd R. Quackenbush*
Continuum Dynamics, Inc., Princeton, New Jersey
Donald B. Bliss†
Duke University, Durham, North Carolina
and
Daniel A. Wachspress‡
Continuum Dynamics, Inc., Princeton, New Jersey

Free-wake analyses of helicopter rotor wakes in hover using time stepping have been shown to encounter instabilities which preclude convergence to valid free-vortex solutions for rotor-wake geometries. Previous work has demonstrated that these convergence difficulties can be overcome by implementing a new free-wake analysis method based on the use of influence coefficients. The present paper reviews this approach and documents its incorporation into a hover performance analysis called Evaluation of Hover Performance using Influence Coefficients (EHPIC). The technical principles underlying the EHPIC code are described with emphasis on steps taken to develop the single-filament wake models used in previous work into a multifilament wake valid for realistic hover performance predictions. The coupling of the wake model to a lifting surface loads analysis is described, and sample problems are solved that illustrate the robustness of the method. Performance calculations are also undertaken for hover to illustrate the utility of EHPIC in the analysis of rotorcraft performance.

Nomenclature

b = binormal unit vector at a collocation point
n = normal unit vector at a collocation point
q = vector of cross-flow velocities at each collocation point
Δq_b = perturbation in binormal component of q
Δq_n = perturbation in normal component of q
$\tilde{Q}_{(\,)(\,)}$ = influence coefficient submatrices
r = radial distance from rotor hub
r_f = radius of far wake
t = tangent unit vector at a collocation point
w = velocity normal to rotor blade surface at a control point
w_f = downwash velocity in the far wake
x = vector of collocation point position
Δx_b = perturbation of collocation point position in binormal direction
Δx_n = perturbation of collocation point position in normal direction
γ = vector of bound circulation of each vortex quadrilateral
Γ = filament circulation
Ω = rotor blade rotation rate (rad/s)

Introduction and Basic Principles

New Approach to the Hover Problem

THE determination of the wake of a hovering rotor poses a particularly challenging computational problem. Previous numerical solutions for the free wake of a hovering rotor[1-4] have experienced stability and convergence problems. The instability encountered causes the wake to depart from an idealized, smoothly contracting helical form. This behavior is described in Ref. 1 and was also encountered using the significantly different computational method in Ref. 4. The instability causes residual unsteadiness in the downwash velocity at the rotor blade and, if left unchecked, it may lead to uncontrollable divergence of the solution.

This fundamental difficulty arises because the wake of a hovering rotor actually is unstable, as has been confirmed by experiment. The instability can be viewed as the first step in the evolution from an orderly flow structure near the rotor to a turbulent jet far below. The unstable behavior observed computationally for rotor wakes is also closely related to the instability observed in analytical treatments of vortex helices,[5,6] which revealed a wide range of unstable modes of motion in both single and interdigitated helices. A linearized analyses of these solutions indicated that any perturbation of the self-preserving helical solution would produce divergent oscillations in time domain computations.[7]

The common feature of the preceding free-wake hover analyses is that they seek to find the solution through just such time marching schemes. Starting with an incorrect initial wake configuration, the subsequent wake motion is computed in the hope that it will progress to the desired hover solution. However, because of the wake instability, it is not possible to obtain an equilibrium solution for the wake structure using a time marching approach. Researchers have tried to circumvent this stability problem by artificial suppression of the instability. Methods of suppression include periodically smoothing and imposing symmetry on the wake and the introduction of substantial amounts of numerical damping. Unfortunately, such approaches may effectively impose forces on the wake leaving open the question of whether equilibrium-free motion conditions are really being satisfied. Depending on the type of suppression used, long computer run times may still be required to obtain convergence or to compute time-averaged results if some residual instability remains.

In order to circumvent the limitations of the traditional approach, a new method for finding solutions to the hover problem was proposed several years ago.[7] This new approach is based on the proposition that the free-wake hover problem possesses a self-preserving steady solution when viewed in

Received Nov. 17, 1988; revision received May 19, 1989.

*Senior Associate. Senior Member AIAA.
†Associate Professor, College of Engineering, Department of Mechanical Engineering and Materals Science. Member AIAA.
‡Associate.

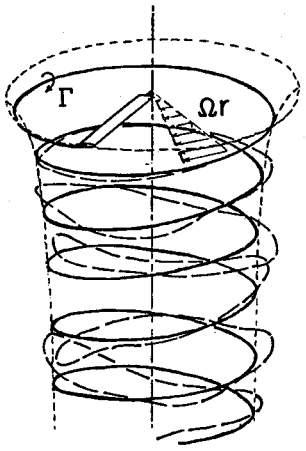

Fig. 1 Ideal rotor wake solution (solid line) vs typical wake instability (dashed line).

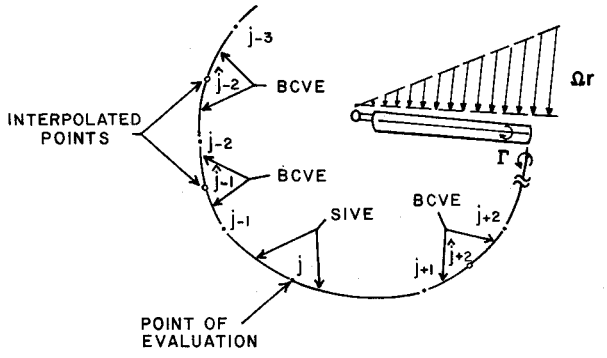

Fig. 2 Typical arrangement of elements to calculate the velocity at a point in the wake.

blade-fixed coordinates. The self-preservation property of this ideal solution is not to be confused with its stability; in fact, the solution has been demonstrated to be unstable. Despite this fact, the solution can be found by an influence coefficient method which does not involve temporal evolution and which can be used even though the solution itself is unstable.

Bliss et al.[7] demonstrated the new solution method for a simple tip vortex wake trailed from blades with prescribed circulation. The present paper deals with the application of this method to the development of a complete analysis of the full-span hover wake coupled to a blade aerodynamics analysis. The resulting code, called Evaluation of Hover Performance using Influence Coefficients (EHPIC), is capable of producing unambiguously converged free wakes and of predicting the aerodynamic performance of rotor configurations with very good accuracy.

Influence Coefficient Solution Method

The wake of a hovering rotor possesses a self-preserving solution when viewed in a coordinate system rotating with the blade. This solution for a wake composed of a single tip vortex is sketched in Fig. 1. Bliss et al.[4] used a time-dependent scheme in the rotating reference frame and encountered the usual wake instability also sketched in Fig. 1. This wake instability develops about the steady self-preserving solution, and it is really from this standpoint that the instability should be studied.

From the standpoint of performance prediction, the problem is to find the wake solution which is self-preserving and stationary in blade-fixed coordinates. The desired solution can be obtained by a mathematical procedure which requires that each vortex filament satisfy the condition that the wake shape be self preserving. In practice, the solution must be obtained

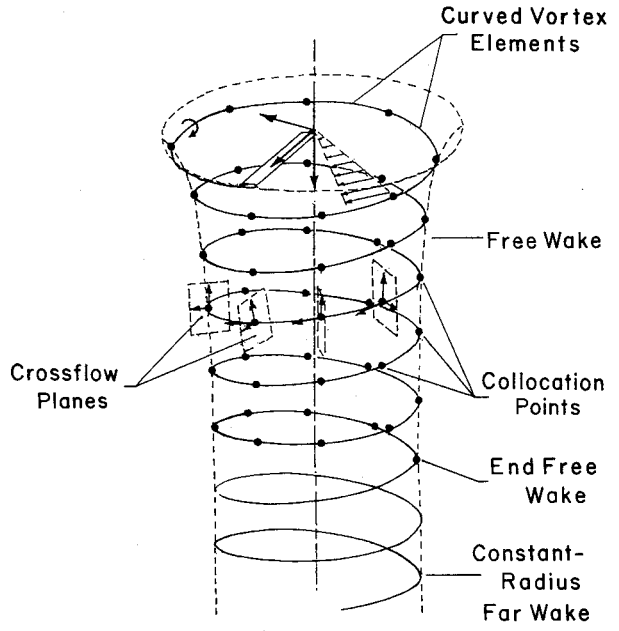

Fig. 3 Tip-vortex wake represented by curved-vortex elements showing the crossflow planes at collocation points and the two-part wake model.

numerically, which means that the wake must be modeled using discrete vortex elements. The location of each vortex element is defined by a set of collocation points which connect the vortex elements. The wake shape is modified by changing the locations of these points. To find the physically correct solution, it is necessary to locate the collocation points so that the net velocity vector at each point is tangent to the vortex filament curve passing through this point.

The vortex-induced velocity field is obtained by evaluating the Biot-Savart integral over both the vortex wake and the bound circulation on the blades. To model the wake, the curved vortex elements described in Refs. 4, 7, and 8 are used. The Basic Curved Vortex Element (BCVE) is used to evaluate the velocity contribution at any point in the flow field not on the element itself (traditionally, straight line elements have been used for this purpose). The Self-Induction Vortex Element (SIVE) is used to evaluate the velocity induced by a vortex on itself. Figure 2 shows how these two types of curved elements are used to represent a filament. The relatively smooth, closely spaced curves that describe the vortex shapes in hover are ideally suited for the use of curved elements. Furthermore, different size elements can be used together without discontinuities, thereby providing different degrees of resolution in different parts of the wake.

From a given set of collocation point locations for each filament, the local tangent, normal, and binormal vectors at each collocation point are determined. The local normal and binormal vectors can be used to define a crossflow plane at each collocation point, as shown in Fig. 3. If the total velocity at any point has a component in its crossflow plane, then the solution cannot be steady, since the vortex filament would then be convected in the crossflow plane.

The solution procedure, which involves a way to systematically reduce the crossflow velocity to zero at every collocation point, can now be described. (Assume for the moment that the strength and location of each filament leaving the blade is held fixed; the coupling to the blade aerodynamics will be described later once the wake treatment is understood.) The effect of small displacements of each collocation point on the velocity at every other collocation point and the displaced point itself are first determined. For example, for a small displacement of the jth point in the local binormal direction, the resulting small velocity changes in the normal and binormal directions

of every point (including point j) are computed. For sufficiently small displacements, the effect is essentially linear, and a proportionality constant, or influence coefficient, relating each velocity perturbation to the displacement can be calculated. This process is repeated for the displacement of point j in the local normal direction. The effect of any small displacements of point j in the local crossflow plane can then be calculated at every other point. After repeating this process for all free wake points ($1 \leq j \leq N$) in both the normal and binormal directions, an influence coefficient matrix relating crossflow velocity perturbations to small displacements from a given wake configuration has been established.

In addition to the wake effects described just above, it is necessary to include the velocity contributions due to the bound circulations on the rotor blades, any axial (climb) velocity component, and the rotating frame velocity magnitude Ωr. Also, coefficients must be determined for the influence of changes in blade bound circulation on the wake crossflow velocities, and the downwash velocities at the blade. This process is summarized below and described in detail in Ref. 9.

For a given arrangement of the free wake collocation points, the net velocity in each crossflow plane can be computed. To move toward the desired solution, the collocation points must be displaced so as to reduce these crossflow velocities. This process is illustrated in Fig. 4. The influence coefficient matrix can be used to predict the set of collocation point displacements which will reduce all of the crossflow velocities. If the wake flowfield problem were linear, only a single matrix inversion would be required to obtain the solution. Since the wake problem is actually nonlinear, the procedure involves a relaxation process in which the solution is reached through a series of quasilinear steps.

It should be emphasized that the repeated application of the preceding procedure does not correspond to time stepping. In this quasilinear relaxation process, the collocation points are moved to reduce the crossflow velocities, rather than being moved in the directions indicated by the crossflow velocities. Thus, the successive displacements obtained from repeated applications of the influence coefficient method do not correspond to a physical motion of the wake. This is one reason why stability of the physical flowfield is not a requirement for the influence coefficient method to work.

It should also be emphasized that the approach just described is restricted to cases where an ideal, steady, self-preserving solution can be found. This restriction limits the applicability of the method to rotors in hover and axial flight where the solution is steady in the rotating frame. This solution method is not applicable to forward flight since there is no reference frame in which the flowfield can be made to appear steady. Conversely, of course, this approach can be applied to the analysis of fixed-wing wakes in forward flight or any vortex-dominated flow where a steady solution exists.

Note that there is a strong similarity between the matrix operations used in the method just described and those employed in lifting surface theory. Because of this, the wake solution method and a blade-lifting surface theory can be combined and solved simultaneously. This is one of the advantages of the present approach, as will be described below.

Far Wake Implementation

A free wake analysis necessarily involves only a finite number of turns of discrete filamentary vortices. Beyond the free-wake region, the wake must be continued using a far-wake model if the solution is to be physically correct. The free-wake region is composed of a number of filaments trailed from the primary blade to simulate the tip vortex, inboard sheet, and the root vortex. Other blades and their wakes are assumed to have the identical configuration since the ideal solution will have blade-to-blade symmetry, and these are handled by an equivalent image system. It is necessary, though, to continue the free-wake region with a far-wake model. The far-wake model used in the current-hover analysis code is an idealized extension of the free wake. The free-wake filaments are continued as ideal discrete helices whose spacing may be determined either by momentum theory or the free-wake spacing, at the option of the user.[9] (See Fig. 3 for a schematic of a simple tip-vortex-only case.) If care is taken to insure that the far wake is attached after the wake contraction is complete, it should be very nearly force free.

Lifting-Surface Analysis

In order to calculate the average performance characteristics of the rotor blade, a lifting-surface analysis of the blade-circulation distribution has been included in the solution method. Lifting surface methods similar to the one used here have been widely used in the computation of flow around aircraft of complex configurations. These methods use a distribution of sources, doublets or vortices, or different combinations of these entities arranged in a variety of geometrical forms. The rotor blade is represented in the present work by a surface consisting of vortex quadrilaterals. This model solves for the set of bound circulation values that enforce flow tangency (i.e., zero downwash) at the control points at the center of the quadrilaterals. The vortex quadrilateral method was chosen because the unknown circulations of the vortex quadrilaterals can be easily solved for using the influence coefficient approach which has been employed for calculating the wake. The lifting-surface and free-wake problems are thus combined into one calculation and can be solved simultaneously as described below. Also, the vortex quadrilateral representation was readily integrated geometrically into the existing trailing vortex filament model of Ref. 7.

The vortex quadrilateral method has several limitations shared by many current panel methods. The method is based on potential flow theory for an incompressible flow. Approximate subsonic compressibility corrections have been added to account for subcritical compressibility effects, and viscous effects have also been approximated by including two-dimensional drag coefficients (see below). The present formulation is inadequate for treating leading-edge and blade-tip separations.

Formulation of Blade/Wake Coupling

Now that the blade aerodynamic model has been introduced, the mathematical form of the coupled-wake relaxation can be discussed. For the purposes of illustration, the case of a wake composed of a single constant-strength vortex filament is considered first (i.e., the coupling to the blade aerodynamic load is ignored for the moment). The more general case of a multiple-filament wake with explicit coupling to the blade load is discussed below.

Given that q_n and q_b denote the normal and binormal components, respectively, of the velocity field at the wake collocation points, the linearized derivatives or influence coefficients

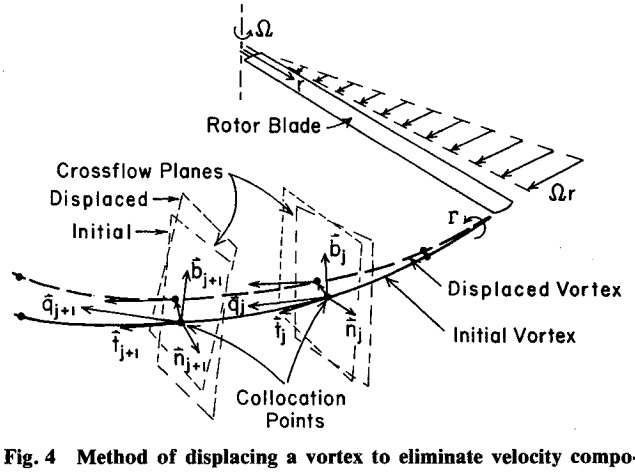

Fig. 4 Method of displacing a vortex to eliminate velocity components in planes normal to the vortex curve. Equilibrium state is zero crossflow velocity in every plane.

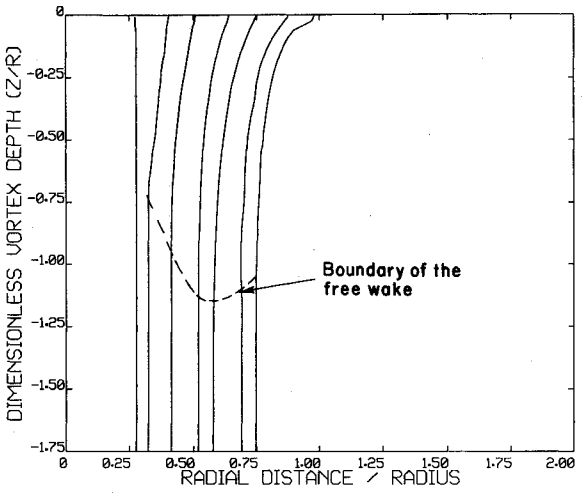

Fig. 5 Wake geometry of a representative two-bladed rotor using seven free filaments (thrust coefficient = 0.0041).

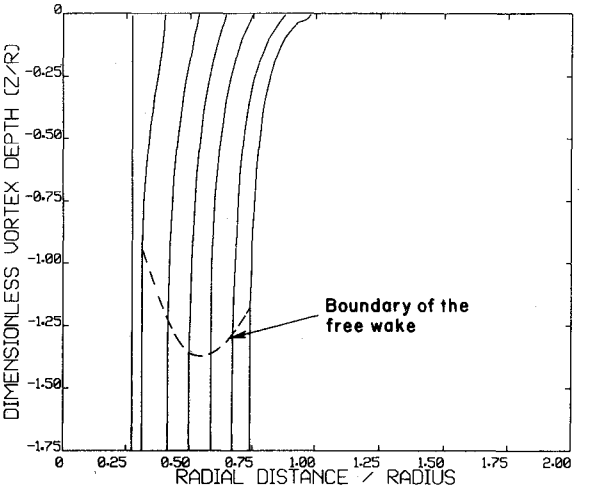

Fig. 6 Wake geometry of a representative four-bladed rotor using seven free filaments (thrust coefficient = 0.0068).

associated with the single-filament wake can be expressed as follows:

$$\tilde{Q}_{nn} = Q^{ij}_{nn} = \frac{\partial q_{n_i}}{\partial n_j} \tag{1a}$$

$$\tilde{Q}_{nb} = Q^{ij}_{nb} = \frac{\partial q_{n_i}}{\partial b_j} \tag{1b}$$

$$\tilde{Q}_{bn} = Q^{ij}_{bn} = \frac{\partial q_{b_i}}{\partial n_j} \tag{1c}$$

$$\tilde{Q}_{bb} = Q^{ij}_{bb} = \frac{\partial q_{b_i}}{\partial b_j} \tag{1d}$$

for $1 \le i \le N$ and $1 \le j \le N$, where N is the number of free-wake points. Note that these coefficients denote the effect of displacing the jth point on the velocities at the ith point; they define the influence coefficient matrices. The velocity change vectors are related to the change of displacement vectors through the influence coefficient matrices, namely

$$\tilde{Q}_{nn}\Delta x_n + \tilde{Q}_{nb}\Delta x_b = \Delta q_n \tag{2a}$$

$$\tilde{Q}_{bn}\Delta x_n + \tilde{Q}_{bb}\Delta x_b = \Delta q_b \tag{2b}$$

To obtain zero net crossflow velocity, it is necessary to choose the point displacements so that the velocity changes cancel the net crossflow velocity. Therefore

$$\Delta q_n = -q_n \qquad \Delta q_b = -q_b \tag{3}$$

Equations (2) and (3) can now be solved simultaneously for the change of displacement vectors Δx_n and Δx_b. The colocation points are displaced by Δx_b and Δx_n to obtain a new-wake shape. Since the wake problem is nonlinear, this process must be repeated several times.

The previous discussion has shown how the relaxation process proceeds for a single, constant-strength filament. To couple in blade aerodynamics, we start with the general statement that $q = f(x,\gamma)$ and $w = h(x,\gamma)$ where $q = (q_n, q_b)$, the vector of normal and binormal velocities at the wake collocation points, and w represents the vector of downwash velocities at the blade-control points. The vectors representing the independent variables in the problem are x and γ, the collocation point positions and the bound-circulation values, respectively. As discussed previously, the calculation is designed to find the values of x and γ for which the dependent variables q and w are nulled. The form of the complete set of influence coefficient equations is

$$\begin{bmatrix} \Delta q_n \\ \Delta q_b \\ \Delta w \end{bmatrix} = \begin{bmatrix} \tilde{Q}_{nn} & \tilde{Q}_{nb} & \tilde{Q}_{n\gamma} \\ \tilde{Q}_{bn} & \tilde{Q}_{bb} & \tilde{Q}_{b\gamma} \\ \tilde{Q}_{wn} & \tilde{Q}_{wb} & \tilde{Q}_{w\gamma} \end{bmatrix} \begin{bmatrix} \Delta x_n \\ \Delta x_b \\ \Delta \gamma \end{bmatrix} \tag{4}$$

In Ref. 7, only the submatrices $\tilde{Q}_{nn}$, $\tilde{Q}_{nb}$, $\tilde{Q}_{bn}$, and $\tilde{Q}_{bb}$ were calculated since the blade-bound circulation values were not degrees of freedom; their introduction requires the calculation of the remaining submatrices. These are found in very much the same way as the wake-on-wake influence coefficients, though the programming logic is somewhat simpler.

To sum up the discussion to this point, the influence coefficients show the effect of linearly small changes in wake displacements on all the colocation points. In a linear sense, the changes in displacements required to null wake-crossflow velocities can be found by solving this linear system. It is important to note, however, that since the system is not truly linear, the solution process must be repeated a number of times using updated velocities and influence coefficients. Also, before proceeding further, the generality of the technical approach just described should be reemphasized. While the motivation for this work sprang largely from the desire to improve the treatment of helicopter rotors in hover, the influence coefficient method developed here may be applied to any vortex-dominated flowfield which possesses a steady solution in some reference frame. This class of problems includes rotors in climb, propellers and propfans in forward flight, wind turbines in an axisymmetric freestream, as well as lifting wings in rectilinear flight or in flight with steady angular rates.

Special Features of the Wake Model

Multifilament Wakes

The work documented in Ref. 7 demonstrated that converged free-wake geometries could be found for hover wakes with single, fixed-strength trailing filaments. The primary purpose of this work, as noted earlier, was to develop new techniques to allow the performance of more realistic hovering rotors to be analyzed. This section will describe the results of representative model problems using multifilament wakes and will document some of the special features of the model developed to date.

The model problems to be presented will show converged wake geometries for both two-bladed and four-bladed rotors trailing seven filaments. This model assumes an essentially

instantaneous rollup of the tip vortex and uses the six inboard filaments as a model of the more diffuse inboard wake. The trailing filaments use between two and three turns of free wake each. The vortex quadrilateral layout on the blade features 30 quads spanwise and one chordwise. These parameters were chosen for the purpose of performing representative calculations; Ref. 9 addresses the proper choices to be made for actual rotors, though for conventional planforms this particular choice is usually quite appropriate.

Figure 5 shows the converged wake geometry for a two-bladed rotor. Note that the filaments in the free-wake region near the blade all merge smoothly with the far wake. The trajectory of the tip filament near the blade shows a slight kink, reflecting the change in vortex descent rate that occurs after the first encounter with a rotor blade. Figure 6 shows the same blade and wake model at the same collective, but now with a four-bladed rotor. The qualitative nature of the wake geometry is the same, though the four-bladed case features more rapid radial contraction of the tip vortex due to the higher thrust. Also, note that the boundary of the free-wake region has moved down relative to the two-bladed case; since both the two- and four-bladed cases use the same number of turns of free wake in each filament, this difference directly reflects the increased downwash in the four-bladed case. Both of these cases, though, are indicative of the smooth, well-behaved wake geometry typically found using the EHPIC code.

Azimuthal Variation of Arc Size

As may be inferred from the discussion of fundamental principles earlier, the wake relaxation in this solution method proceeds in what is essentially an Eulerian frame defined by curvilinear coordinates along each filament. In these calculations, the collocation points are not associated with any particular fluid particles, unlike the Lagrangian time-stepping approach used in previous free-wake analyses.[1,2] Rather, they represent the trajectory of the centroid of the vorticity distribution trailed from that portion of the blade span from which the filament was generated.

This circumstance also opens up a new set of possibilities for the relaxation approach used here. In Lagrangian calculations, the azimuthal spacing of the collocation points is rigidly tied to the time step chosen for the calculation, so there is strong motivation to minimize the number of steps around the azimuth so as to minimize the computation time. However, large time steps lead to coarse wake structure that is incapable of resolving finescale events like blade-vortex interaction. Lagrangian methods thus have a built-in conflict between computational efficiency and accuracy of resolution of the flow.

The relaxation method used here enjoys far more flexibility. Because of the independence of the method from any fixed time step, the collocation points may be laid out in unequal azimuthal spacings. This circumstance permits points in the wake to be closely spaced near the rotor blades, where detailed resolution of the wake structure is likely to be important, while far-wake turns use very coarse spacing (as few as four elements per turn) to minimize computation time.

Two simple but representative model problems suffice to illustrate this capability. Figure 7 shows the trajectory of a tip filament from a simple two-bladed rotor. In this example, the blade trailed a single free filament, consisting initially of 24 45-deg curved elements. This baseline run was then modified by subdividing the first arc into smaller subarcs: first, two 22.5-deg arcs; then, three 15-deg arcs; and finally, four 11.25-deg segments. In each case, the rotor collective pitch was adjusted to keep the thrust coefficient on the rotor constant. (The required changes in collective pitch were never more than a half of a degree, so the flow tangency condition at the blade/wake connection points did not vary significantly between cases.) As Fig. 7 shows, the trajectory of the tip filament moves upward as the first element is refined. The filament shows a strong tendency to converge to a final position as the number of subarcs increases. Further refinement of the arcs would not be appropriate since this would require resolving the rollup of the tip vortex from the side and trailing edges of the blade; the analysis discussed here cannot resolve this process reliably, but follow-on versions are being developed to attack this problem. The total vertical displacement in this refinement process is only a few percent of rotor radius, but this is a significant fraction of the original displacement below the rotor plane. In rotors with large numbers of blades where blade vortex interaction is an issue, such refinement can have an important effect on blade-load predictions.

The fundamental phenomenon at work here is that the vortex experiences a steep gradient in downwash as it moves away from the blade. The velocity induced by the bound circulation falls off rapidly, but if the filament is modeled with large arcs, it will be "thrown down" in a direction tangent to the chord line of the blade section from which it is trailed. As smaller arcs are introduced downstream of the blade, the downwash gradient will be resolved and the filament will relax smoothly to its proper trajectory.

Clearly, it is desirable to use a large number of arcs on those portions of filaments passing near blades so that blade/vortex interactions can be correctly resolved. An example of this procedure is shown in Fig. 8. Here, the same two-bladed rotor has been used, again with a single filament trailing from each blade. The baseline case for the tip filament uses 45-deg arcs;

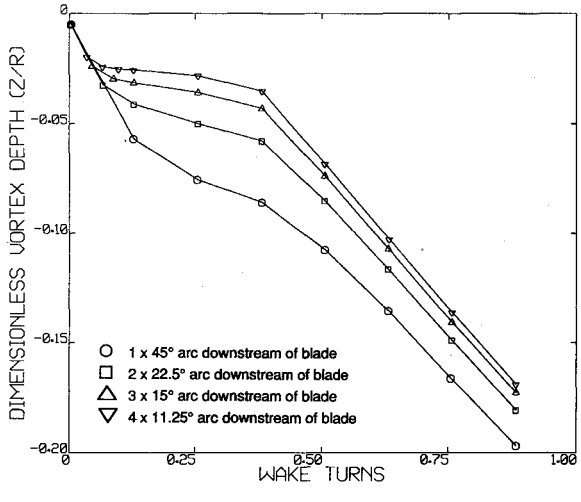

Fig. 7 Effect of refining the modeling of the first element of the tip vortex on the overall filament trajectory.

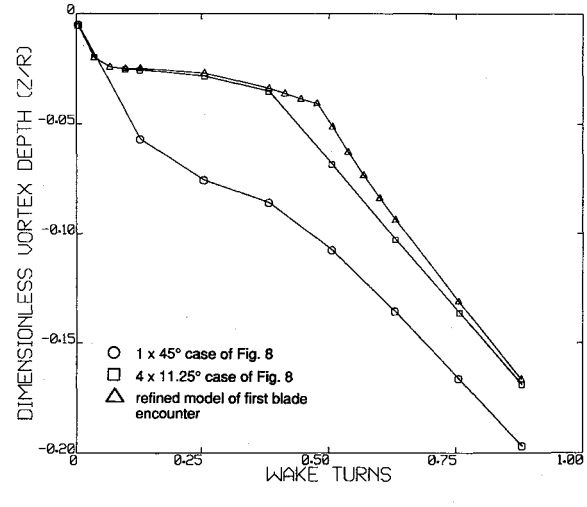

Fig. 8 Effect of further refining the case of Fig. 8 using 8- × 11.25-deg arcs in the vicinity of the following blade.

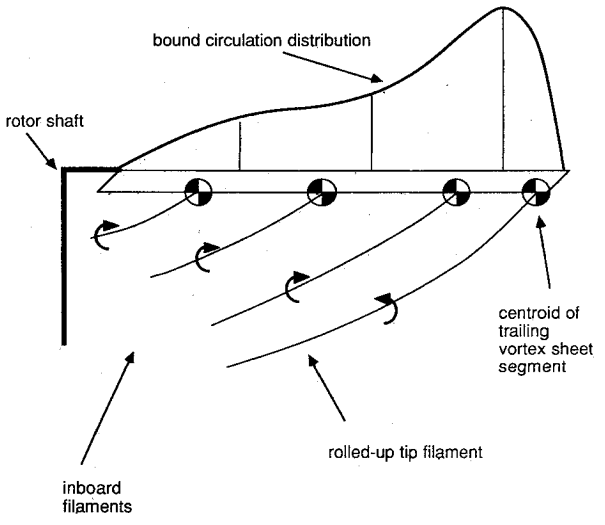

Fig. 9 Schematic of vortex filaments trailing from centroids of vortex sheet segments trailing from the rotor blade.

subdividing the first element into four arcs as above shifts the filament upward. Then, the filament is further refined in the vicinity of the following blade by subdividing the two elements immediately adjacent to the blade. As is evident, the trajectory in the vicinity of the blade changes significantly, though it converges once again to the unrefined arc trajectory as it moves further downstream.

Strength and Release Points of Free Filaments

As discussed in the previous sections, the current analysis models the wake of a hovering rotor as a set of curved vortex filaments. In reality, the wake leaves the blade as a continuous vortex sheet, though the tip region typically begins to roll up rapidly a short time after being trailed. The ideal approach to the simulation of the wake and its rollup would be to use freely distorting, curved-sheet elements that could smoothly merge into the appropriate trailing wake. In practical terms, however, the only realistic tools for use in this type of hover analysis are vortex filaments.

Given that filaments must be used, it appears desirable to use a large number of them so that the full sheet would be correctly modeled in the limit. However, the problems attending the use of a large number of point vortices to simulate a two-dimensional sheet have been well documented. The analogous difficulties in three dimensions are 1) very short elements must be used to resolve the rollup of the vortices leading to long computation times and 2) that the individual filaments must be smoothly amalgamated as rollup proceeds. These issues, particularly the second, cannot currently be resolved except by ad hoc approximations.

In the face of these difficulties the traditional approach and the one adopted here have been to use a relatively small number of discrete filaments (no more than 10 or 12) to model the wake of each blade. Fortunately, the typical wake structure of conventional rotors is well suited to this approximation. The wake of most rotor blades resolves itself into a strong tip vortex and a more diffuse inboard sheet which can be successfully modeled by several discrete filaments with appropriately chosen cores. When using such models, care must be taken to choose the filament strengths and release points so as to preserve as much of the original character of the continuous wake sheet as possible. Reference 9 describes the "overlap wake" model that smooths the velocity field in the extreme near wake.

Figure 9 shows a schematic of a typical load distribution on a rotor blade and a wake assumed to consist of four free filaments. In practice, the user has the option of choosing the boundaries of circulation zones on the blade. The strengths of the filaments trailing from these regions are then defined to conserve the strength of each sheet segment. To provide a consistent physical basis for the choice of trailer locations, approaches similar to that described for fixed-wing wakes in Ref. 10 may be used. In this reference, a model (originally developed by Betz) is described that conserves the centroid of vorticity in the trailing wake during the roll up of wingtip vortices. Positioning the rolled-up wake in accordance with the demands of centroid conservation removes a degree of arbitrariness from the process of locating the wake filaments. In the context of the hovering rotor problem, the bound circulation distribution is divided into sections by the user, as shown in Fig. 9. The radial location of the filament is chosen to conserve the integral invariant for axisymmetric distributions of vorticity derived by Batchelor in Ref. 11.

Cutoff Distance and Core Size for Filaments

It is believed that an analytical treatment of the wake rollup using a Betz-type model provides the best results within the context of the current method. In this approach, each portion of the trailed vortex sheet is assumed to roll up around the sheet centroid location. The portion of the sheet that rolls up into a tip vortex is determined by the location of the maximum circulation for most conventional rotor designs. However, if a finite-strength vortex filament of infinitesimal cross section is used, then the Biot-Savart integration is logarithmically singular when the point of evaluation is placed on the curved filament itself. This problem is avoided by stopping the integral at a cutoff distance on either side of the point of evaluation. The cutoff distance used for this resultant filament is based on the method of Ref. 12, which utilizes blade-loading information to define the cutoff distance parameters.

The self-induced velocity of the inboard filaments is also handled by a cutoff distance approach. It can be shown that a curved segment of vortex sheet experiences a self-induced velocity, similar in principle to that experienced by a vortex core. A planar, constant-strength, curved vortex sheet can be shown to have a cutoff distance equal to half the sheet width. In the analysis, the half-width, cutoff distance formula is used for inboard filaments.

A choice for tip vortex core radius that is consistent with the approach for cutoff distance just described is to pick the radius to equal the distance from the inboard edge of the tip vortex sheet to the centroid of the trailing vortex distribution. For the inboard filaments representing the trailing sheet, the proper choice is half the width of the portion of the sheet that the filament represents (this coincides with the inboard filament cutoff distance). Uniform vorticity cores are assumed for all filaments.

Performance Analysis

Rotor Performance Evaluation

As described in the preceding sections, the relaxation solution generates the appropriate bound circulation values to satisfy the flow tangency condition at each of the blade-control points. Given these bound circulation values and a complete description of the velocity field at the blade, the Joukowski law may be used to compute the forces on each vortex quadrilateral. This procedure is repeated for each quadrilateral, and the results are summed to provide the total thrust and induced torque.

During the computation of the thrust on the blade, the incremental thrust on each chordwise quad at a given radial station is summed to give the spanwise lift distribution. Using the c_ℓ so obtained along with the local Mach number, two-dimensional airfoil section data are consulted to provide the local profile drag coefficient. Compressibility, viscosity, and thickness effects are thus incorporated into the profile torque at each section.

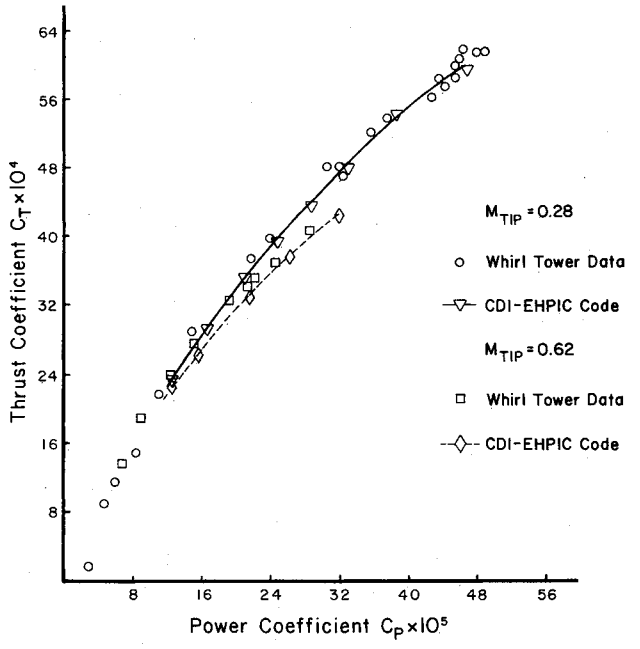

Fig. 10 Performance predictions for a two-bladed, full-scale rotor (data from Ref. 13).

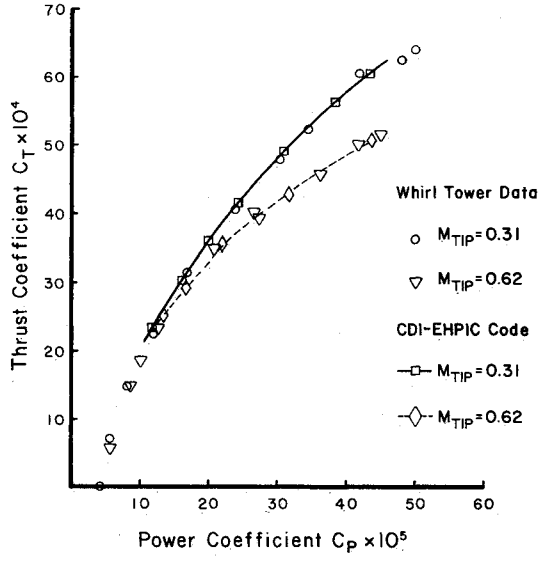

Fig. 11 Performance predictions for a three-bladed, full-scale rotor (data from Ref. 14).

Performance Correlations with Experimental Data

To carry out preliminary validation of the EHPIC code, two rotor systems were chosen for experimental correlation studies. The two test cases discussed here were run with 30 vortex quadrilaterals spanwise and a single quadrilateral chordwise. Subsequent checks using more refined meshes indicated relatively small differences in predicted performance; however, such refined meshes may well be necessary for more complex planforms.

Reference 13 contains thrust and power data for a full-scale, two-bladed rotor. The blades were untapered and had a radius of 8.17 m (26.8 ft) and a chord of 0.58 m (1.91 ft). The blades featured 8 deg of linear twist and were tested at tip Mach numbers between 0.28 and 0.66. The blades also used the NACA 0012 section across the full rotor span. Figure 10 shows the agreement achieved for two tip Mach numbers: 0.28 and 0.62. The agreement is generally favorable over the entire range of performance surveyed.

Reference 14 gives thrust and power information on a three-bladed rotor with partial span taper. The rotor had a radius of 5.8 m (19 ft) with a constant chord of 0.32 m (1.04 ft) out to 55% of radius, tapering to 0.17 m (0.56 ft) at the tip. The NACA 23015 airfoil section was used across the entire span. The blades used 8 deg of linear twist. Figure 11 shows the correlation achieved for this tapered rotor for tip Mach numbers of 0.31 and 0.62. Again, the correlation is good even at very high thrust levels.

Obviously, it is of interest to examine the ability of the EHPIC code to predict the hover performance of a wide range of rotorcraft configurations. This is undertaken in a study by Felker et al.[15] where the performance of rotors with a variety of twist, taper, and other planform variations are considered.

Conclusions

The development of the EHPIC code was an outgrowth of the initial work on the influence coefficient approach to free-wake hover analysis described in Ref. 7. The major objective of the current effort was to determine if the approach that was successful for the simplified rotor wakes analyzed in Ref. 7 could be extended to handle realistic rotor wakes and to provide reliable performance predictions for rotors in hover and axial flight. As documented herein, this effort has been highly successful. The original model has been upgraded to include as many as 11 trailing filaments per blade. The wake geometry solution has been coupled to a vortex-lattice, lifting-surface model of the blade that relaxes the bound circulation at the same time as the filament trajectories. The performance calculations undertaken using this free-wake model have demonstrated good correlation with representative rotors. Also, unlike previous Lagrangian free-wake analyses, the EHPIC code is capable of handling filaments with variable arc size, a feature which allows selective refinement of the wake model in regions requiring high resolution (e.g., near rotor blades).

Several features of the EHPIC code could benefit from additional refinement in future development. The computational efficiency of the routine could be enhanced by more systematic use of approximations for curved elements in the far field. Also, the rollup of the tip vortex and the inboard filaments could be modeled in more detail with more attention to the sheetlike structure that may be present in some cases as well as to explicit computation of the vortex rollup. Finally, a lift stall model should be incorporated into the current lifting-surface analysis to enhance confidence in performance predictions at high thrust.

Even without these refinements, however, the EHPIC code represents a significant new development in rotary-wing aerodynamics. Its novel approach to the calculation of the free vortex wakes of hovering rotors has been successfully applied to the prediction of the performance of a variety of designs. The results documented in this paper have shown it to be a flexible, accurate, and practical tool for the analysis of advanced rotorcraft.

Acknowledgment

This research was supported by NASA Ames Research Center under Small Business Innovation Research Contract NAS2-12148. The NASA technical monitor was F. F. Felker.

References

[1]Landgrebe, A. J., "An Analytical and Experimental Investigation of Helicopter Rotor Hover Performance and Wake Geometry Characteristics," U.S. Army Air Mobility Research Development Laboratory, Moffett Field, CA, USAAMRDL TR 71-24, June 1971.

[2]Scully, M. P., "Computation of Helicopter Rotor Wake Geome-

try and its Influence on Rotor Harmonic Airloads," M.I.T., Cambridge, MA, Aerospace Structures Research Laboratory TR 178-1, March 1975.

[3]Clark, D. R. and Leiper, A. C., "The Free Wake Analysis: A Method for the Prediction of Helicopter Rotor Hovering Performance," *Journal of the American Helicopter Society,* Vol. 15, No. 1, Jan. 1970, pp. 3-11.

[4]Bliss, D. B., Quackenbush, T. R., and Bilanin, A. J., "A New Methodology for Helicopter Free Wake Analyses," presented at the 39th Annual Forum of the American Helicopter Society, Paper A-83-39-75-0000, May 1983.

[5]Widnall, S. E., "The Stability of a Helical Vortex Filament," *Journal of Fluid Mechanics,* Vol. 54, Part 4, 1972, pp. 641-663.

[6]Gupta, B. P. and Loewy, R. G., "Aerodynamic Stability of Multiple, Interdigitated Helical Vortices," *AIAA Journal,* Vol. 12, Oct. 1974, pp. 1381-1387.

[7]Bliss, D. B., Wachspress, D. A., and Quackenbush, T. R., "A New Approach to the Free Wake Problem for Hovering Rotors," *Proceedings of the 41st Annual Forum of the American Helicopter Society,* American Helicopter Society, Alexandria, VA, 1985, pp. 453-469.

[8]Bliss, D. B., Teske, M. E., and Quackenbush, T. R., "A New Methodology for Free Wake Analyses Using Curved Vortex Elements," NASA CR-3958, Dec. 1987.

[9]Quackenbush, T. R., Bliss, D. B., Wachspress, D. A., and Ong, C. C., "Free Wake Analysis of Hover Performance Using a New Influence Coefficient Method," NASA CR-4150, 1988.

[10]Bilanin, A. J. and Donaldson, C. duP., "Estimation of Velocities and Roll-Up in Aircraft Vortex Wakes," *Journal of Aircraft,* Vol. 12, July 1975, pp. 578-585.

[11]Batchelor, G. K., *An Introduction to Fluid Dynamics,* Cambridge University Press, 1967, pp. 517-523.

[12]Bliss, D. B., "Prediction of Tip Vortex Self-Induced Motion Parameters in Terms of Rotor Blade Loading," *Proceedings of the American Helicopter Society National Specialists' Meeting on Aerodynamics and Aeroacoustics,* American Helicopter Society, Alexandria, VA, 1987.

[13]Carpenter, P. J., "Lift and Profile Drag Characteristics of an NACA 0012 Airfoil Section as Derived from Measured Helicopter Hovering Performance," NACA TN 4357, Sept. 1958.

[14]Carpenter, P. J., "Effects of Compressibility on the Performance of Two Full-Scale Helicopter Rotors," NACA TN 2277, Jan. 1951.

[15]Felker, F. F., Quackenbush, T. R., and Bliss, D. B., "Comparisons of Predicted and Measured Rotor Performance in Hover Using a New Free Wake Analysis," presented at the 44th Annual Forum of the American Helicopter Society, Paper A-88-45-75-0000, June 1988.